

# Reduced-Feedback Hybrid Precoding for Wideband mmWave MIMO-OFDM Systems

Po-Heng Chou<sup>1,3</sup>, Jia-Qing Lin<sup>2</sup>, Wan-Jen Huang<sup>2</sup>, and Ronald Y. Chang<sup>1</sup>

<sup>1</sup>Research Center for Information Technology Innovation (CITI), Academia Sinica (AS), Taipei 11529, Taiwan

<sup>2</sup>Institute of Communication Engineering (ICE), National Sun Yat-sen University (NSYSU), Kaohsiung 80424, Taiwan

<sup>3</sup>Bradley Department of Electrical and Computer Engineering (ECE), Virginia Tech (VT), Alexandria, VA 22305, USA

E-mails: d00942015@ntu.edu.tw, elinqing514@gmail.com, wjhuang@faculty.nsysu.edu.tw, rchang@citi.sinica.edu.tw

**Abstract**—In this paper, we propose a feedback-efficient hybrid precoding framework for wideband millimeter-wave (mmWave) multiple-input multiple-output orthogonal frequency-division multiplexing (MIMO-OFDM) systems. To mitigate the high cost of radio frequency (RF) chains and channel state information (CSI) feedback in large-scale antenna arrays, we first construct frequency-flat analog precoders by extracting dominant angle-of-arrival (AoA) and angle-of-departure (AoD) directions from sparse frequency-domain channels. For digital precoding, we design a quantized codebook using the Lloyd algorithm and develop a binary-search-based hierarchical interpolation algorithm that adaptively assigns codewords according to subcarrier correlation. The proposed method achieves sub-linear feedback scaling by reducing the feedback overhead from  $\mathcal{O}(K)$  to  $\mathcal{O}(K/M + \log M)$ , where  $K$  is the number of subcarriers and  $M$  is the pilot spacing. Simulation results demonstrate that the proposed method achieves comparable or superior spectral efficiency and bit error rate (BER) performance to existing clustering and interpolation schemes, while significantly reducing computational complexity and exhibiting robustness under imperfect CSI.

**Index Terms**—Millimeter-wave (mmWave), wideband MIMO-OFDM, hybrid precoding, limited feedback, quantized codebook, hierarchical interpolation.

## I. INTRODUCTION

Millimeter-wave (mmWave) frequency bands (24–52 GHz) [1] have been identified as a key enabler for expanding spectrum resources in future wireless systems. However, fully digital beamforming in large-scale antenna arrays requires a dedicated RF chain per antenna, resulting in high hardware cost and power consumption [2]. Hybrid analog–digital precoding alleviates this issue by decomposing the precoder into a low-dimensional digital precoder and a phase-shifter-based analog precoder [3], [4].

In wideband systems, the feedback overhead for subcarrier-dependent digital precoding typically scales linearly with the number of subcarriers, leading to prohibitive feedback cost and computational complexity when the number of subcarriers is large [5]–[8]. To address this issue, limited feedback schemes exploit frequency-domain correlation across subcarriers.

Existing approaches can be categorized into three types. Interpolation-based methods estimate precoders for non-pilot subcarriers from sparse feedback [7]–[9], but typically rely on

fixed subband partitioning, which fails to capture abrupt channel variations in wideband mmWave systems. Codebook-based schemes reduce feedback overhead via quantization [10]–[12], but often lack flexibility in handling frequency selectivity across subcarriers. Learning-based methods learn compact CSI representations [13]–[18], but require extensive offline training and may suffer from generalization issues under practical deployment.

To overcome these limitations, this paper proposes a synergistic framework for feedback-efficient hybrid precoding in wideband mmWave multiple-input multiple-output orthogonal frequency-division multiplexing (MIMO-OFDM) systems. Specifically, dominant angle-of-arrival (AoA) and angle-of-departure (AoD) paths are extracted to construct frequency-flat analog precoders. A Lloyd-based codebook is employed for digital precoding to enable efficient quantization. Most importantly, a binary-search-based hierarchical interpolation algorithm is developed to detect codeword switching points across subcarriers, achieving fine-grained channel tracking while reducing feedback overhead from linear to sub-linear scaling, with logarithmic complexity enabled by binary search, without requiring fixed subband structures or offline training.

The main contributions of this paper are summarized as follows:

- We design analog precoders and combiners by extracting dominant AoA/AoD paths, achieving low-complexity and robust beamforming.
- A Lloyd-based quantized codebook is developed to enable efficient limited-feedback digital precoding.
- A binary-search-based hierarchical interpolation algorithm is proposed to enable adaptive subcarrier partitioning with sub-linear feedback scaling.
- The proposed framework achieves a favorable tradeoff among spectral efficiency, feedback overhead, and computational complexity, with significant feedback reduction compared to fixed-interval baselines.

## II. SYSTEM AND CHANNEL MODELS

Consider a mmWave massive MIMO-OFDM system, as illustrated in Fig. 1, where the transmitter is equipped with  $N_t$  antennas and  $N_t^{\text{RF}}$  RF chains ( $N_t^{\text{RF}} \leq N_t$ ) and the receiver employs  $N_r$  antennas and  $N_r^{\text{RF}}$  RF chains ( $N_r^{\text{RF}} \leq N_r$ ). The signal is transmitted over  $K$  subcarriers with  $N_s$  spatial streams conveyed over each subcarrier and  $N_s \leq$

This work was supported in part by the Academia Sinica (AS) under Grant 235g Postdoctoral Scholar Program, and in part by the National Science and Technology Council (NSTC) of Taiwan under Grant 113-2926-I-001-502-G, 113-2221-E-110-059-MY3, and 114-2218E-110-005.

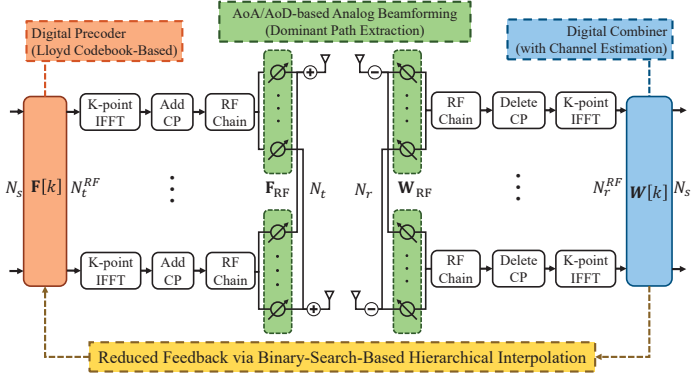


Fig. 1: Proposed reduced-feedback hybrid precoding framework, where AoA/AoD-based analog beamforming, Lloyd-based codebook selection, and binary-search-based hierarchical interpolation jointly reduce feedback overhead.

$\min(N_t^{\text{RF}}, N_r^{\text{RF}})$ . In a conventional wideband hybrid precoding scheme, a digital precoder is allocated to each subcarrier to enhance spectrum efficiency. By leveraging the spectral correlation of the wideband channel, we proposed a hierarchical interpolation with an adaptive subcarrier partitioning to simplify the design of digital precoders over a large number of subcarriers, as illustrated in Fig. 1.

Let  $\mathbf{s}[k] \in \mathbb{C}^{N_s \times 1}$  denote the transmitted signal over the  $k$ -th subcarrier, and  $\mathbb{E}[\mathbf{s}[k]\mathbf{s}^H[k]] = \frac{P}{KN_s} \mathbf{I}_{N_s}$ , where  $P$  is the total transmit power. The data vector over each subcarrier is first passed through a digital baseband precoder  $\mathbf{F}[k] \in \mathbb{C}^{N_t^{\text{RF}} \times N_s}$  to shape the signal. After digital precoding, signals are transformed to the time domain and converted to passband signals via RF chains. The analog precoder  $\mathbf{F}_{\text{RF}} \in \mathbb{C}^{N_t \times N_t^{\text{RF}}}$ , implemented with phase shifters [3], [4], applies phase-only adjustments to the transmitted signals subsequently. The baseband equivalent transmitted signal on the  $k$ -th subcarrier is given by

$$\mathbf{x}[k] = \mathbf{F}_{\text{RF}} \mathbf{F}[k] \mathbf{s}[k], \quad (1)$$

where  $\mathbf{F}_{\text{RF}} \in \mathbb{C}^{N_t \times N_t^{\text{RF}}}$  is the analog precoder, and  $\mathbf{F}[k] \in \mathbb{C}^{N_t^{\text{RF}} \times N_s}$  is the digital baseband precoder for subcarrier  $k$ . Notably, each entry in the analog precoding matrix satisfies a constant modulus constraint, i.e.,  $|\mathbf{F}_{\text{RF}}[m,n]| = \frac{1}{\sqrt{N_t}}$ . Specifically, denote  $\mathbf{F}_{\text{RF}}[m,n] = \frac{1}{\sqrt{N_t}} e^{j\theta_{m,n}}$ , where  $\theta_{m,n}$  is a quantized phase from a discrete codebook, for  $m = 1, \dots, N_t$  and  $n = 1, \dots, N_t^{\text{RF}}$ . To ensure a fair power comparison across schemes, the total transmit power across all subcarriers is constrained by

$$\sum_{k=1}^K \|\mathbf{F}_{\text{RF}} \mathbf{F}[k]\|^2 = KN_s. \quad (2)$$

At the receiver, assuming perfect synchronization, the received baseband signal on the  $k$ -th subcarrier is

$$\mathbf{z}[k] = \mathbf{H}[k] \mathbf{x}[k] + \mathbf{n}[k], \quad (3)$$

where  $\mathbf{H}[k] \in \mathbb{C}^{N_r \times N_t}$  denotes the frequency channel response over the subcarrier  $k$ , and  $\mathbf{n}[k] \sim \mathcal{CN}(\mathbf{0}, \sigma_n^2 \mathbf{I}_{N_r})$

denotes the additive white Gaussian noise (AWGN). Due to sparse scattering in mmWave channels [2], [19], dominant AoA/AoD components can be extracted for analog precoder design. Let  $\mathbf{H}(d)$  denote the channel impulse response at delay tap  $d$ , which is given by

$$\mathbf{H}(d) = \sqrt{\frac{\beta N_t N_r}{L}} \sum_{\ell=1}^L \alpha_{\ell} p_{\text{rc}}(dT_s - \tau_{\ell}) \mathbf{a}_r(\phi_{\ell}) \mathbf{a}_t^H(\theta_{\ell}), \quad (4)$$

where  $\beta$  denotes the large-scale path loss,  $L$  is the number of multipath components,  $\alpha_{\ell}$  is the complex gain of the  $\ell$ -th path,  $\tau_{\ell}$  is its delay,  $T_s$  denotes the sampling interval, and  $p_{\text{rc}}(\cdot)$  is typically chosen as a raised cosine filter. The vectors  $\mathbf{a}_t(\theta_{\ell})$  and  $\mathbf{a}_r(\phi_{\ell})$  represent the transmit and receive array response vectors associated with the AoD  $\theta_{\ell}$  and AoA  $\phi_{\ell}$ , respectively [3].

The frequency-domain channel response at the  $k$ -th subcarrier is obtained via a discrete Fourier transform (DFT) [6] as

$$\mathbf{H}[k] = \sum_{d=0}^{D-1} \mathbf{H}(d) e^{-j \frac{2\pi k d}{K}}, \quad (5)$$

where  $\mathbf{H}(d)$  denotes the  $d$ -th tap of the channel impulse response, and  $D$  is the maximum channel delay spread in samples. In addition, we assume that both transmitter and receiver are equipped with uniform linear arrays (ULAs) with inter-element spacing  $d_{\text{ant}}$ . Let  $\lambda$  denote the carrier wavelength. The normalized array response vectors are defined as

$$\mathbf{a}_t(\theta) = \frac{1}{\sqrt{N_t}} \left[ 1, e^{j \frac{2\pi d_{\text{ant}}}{\lambda} \sin(\theta)}, \dots, e^{j \frac{2\pi d_{\text{ant}}}{\lambda} (N_t-1) \sin(\theta)} \right]^T, \quad (6)$$

$$\mathbf{a}_r(\phi) = \frac{1}{\sqrt{N_r}} \left[ 1, e^{j \frac{2\pi d_{\text{ant}}}{\lambda} \sin(\phi)}, \dots, e^{j \frac{2\pi d_{\text{ant}}}{\lambda} (N_r-1) \sin(\phi)} \right]^T. \quad (7)$$

At the receiver, an analog combiner  $\mathbf{W}_{\text{RF}} \in \mathbb{C}^{N_r \times N_r^{\text{RF}}}$  is applied to the received signal to perform phase-only combining. Each entry of  $\mathbf{W}_{\text{RF}}$  satisfies the constant modulus constraint, i.e.,  $[\mathbf{W}_{\text{RF}}]_{m,n} = \frac{1}{\sqrt{N_r}} e^{j\theta_{m,n}}$ , where  $\theta_{m,n}$  is a quantized phase shift,  $m = 1, \dots, N_r$ , and  $n = 1, \dots, N_r^{\text{RF}}$ .

At the receiver, signals are downconverted and processed via digital combining. A digital combining matrix  $\mathbf{W}[k] \in \mathbb{C}^{N_r^{\text{RF}} \times N_s}$  is then applied to recover the transmitted symbols. The resulting output signal at the  $k$ -th subcarrier is given by

$$\mathbf{y}[k] = \mathbf{W}[k]^H \mathbf{W}_{\text{RF}}^H \mathbf{H}[k] \mathbf{F}_{\text{RF}} \mathbf{F}[k] \mathbf{s}[k] + \mathbf{W}[k]^H \mathbf{W}_{\text{RF}}^H \mathbf{n}[k]. \quad (8)$$

It is important to note that the analog precoder  $\mathbf{F}_{\text{RF}}$  and analog combiner  $\mathbf{W}_{\text{RF}}$  are frequency-flat and thus shared across all subcarriers. This poses a trade-off between spatial selectivity and robustness to frequency variation in wideband scenarios. This motivates the design of an effective channel, which is later exploited for hierarchical interpolation and codebook-based precoding. The effective channel is defined as

$$\mathbf{H}_{\text{eff}}[k] = \mathbf{W}_{\text{RF}}^H \mathbf{H}[k] \mathbf{F}_{\text{RF}}. \quad (9)$$

### III. PROBLEM FORMULATION

The effective channel after analog precoding and combining is defined as

$$\mathbf{H}_{\text{eff}}[k] \triangleq \mathbf{W}_{\text{RF}}^H \mathbf{H}[k] \mathbf{F}_{\text{RF}}, \quad (10)$$

where  $\mathbf{H}_{\text{eff}}[k] \in \mathbb{C}^{N_r^{\text{RF}} \times N_t^{\text{RF}}}$  has reduced dimensionality due to hybrid beamforming. The equivalent channel after digital precoding and combining is then given by

$$\mathbf{H}_{\text{eq}}[k] = \mathbf{W}[k]^H \mathbf{H}_{\text{eff}}[k] \mathbf{F}[k], \quad (11)$$

where  $\mathbf{H}_{\text{eq}}[k] \in \mathbb{C}^{N_s \times N_s}$  represents the equivalent channel seen by the  $N_s$  transmitted data streams.

Under Gaussian signaling and perfect synchronization, the achievable spectral efficiency is given by [2]

$$R = \frac{1}{K} \sum_{k=1}^K \log_2 \det \left( \mathbf{I}_{N_s} + \frac{P}{KN_s \sigma_n^2} \mathbf{H}_{\text{eq}}[k] \mathbf{H}_{\text{eq}}[k]^H \right). \quad (12)$$

The joint precoder-combiner design problem is formulated as in conventional hybrid precoding frameworks [3], [6]

$$\max_{\mathbf{F}_{\text{RF}}, \mathbf{F}[k], \mathbf{W}_{\text{RF}}, \mathbf{W}[k]} R, \quad (13a)$$

$$\text{s.t.} \quad \sum_{k=1}^K \|\mathbf{F}_{\text{RF}} \mathbf{F}[k]\|_F^2 \leq KN_s, \quad (13b)$$

$$\|[\mathbf{F}_{\text{RF}}]_{m,n}\|^2 = \frac{1}{N_t}, \quad \forall m, n, \quad (13c)$$

$$\|[\mathbf{W}_{\text{RF}}]_{m,n}\|^2 = \frac{1}{N_r}, \quad \forall m, n. \quad (13d)$$

where constraint (13b) enforces the total transmit power budget across all subcarriers, constraints (13c) and (13d) impose constant modulus constraints on the analog precoder and combiner, respectively. Solving (13a) jointly over all subcarriers is computationally prohibitive due to the high dimensionality of wideband MIMO-OFDM systems, and further exacerbated by the need for frequent CSI feedback across subcarriers.

To tackle these challenges, we propose a feedback-aware hybrid precoding framework that leverages a shared quantized codebook for digital precoding at both transceiver ends, and a hierarchical interpolation strategy to exploit frequency-domain channel correlation, thereby reducing feedback overhead and computational complexity.

### IV. PROPOSED PRECODER AND CODEBOOK DESIGN

Under the mmWave channel model, the frequency-domain channel matrices across all subcarriers share the same AoA and AoD directions, since they are determined by the physical paths in the sparse propagation environment.

#### A. Analog Precoder and Combiner Design

To exploit this structure, we identify the strongest propagation paths as commonly adopted in mmWave hybrid precoding [3], [19] by ranking their power contributions and use their corresponding angles to construct the analog precoder and combiner.

According to Parseval's theorem [20], the energy in the time domain equals that in the frequency domain. Hence, we evaluate the power of the  $\ell$ -th path by accumulating its contribution across all delay taps

$$\gamma_\ell = \sum_{d=0}^{D-1} |\alpha_\ell p_{\text{rc}}(dT_s - \tau_\ell)|^2, \quad (14)$$

where  $\alpha_\ell$  is the complex gain and  $\tau_\ell$  is the delay of the  $\ell$ -th path, and  $p_{\text{rc}}(\cdot)$  denotes the pulse shaping filter.

Then, we select the index of the strongest path for the  $i$ -th RF chain as

$$\mathcal{X}^{(i)} = \arg \max_{\ell \in \mathcal{L}} \gamma_\ell, \quad i = 1, 2, \dots, N_t^{\text{RF}}, \quad (15)$$

where  $\mathcal{L}$  is the set of unassigned path indices, and the selected index  $\mathcal{X}^{(i)}$  is removed from  $\mathcal{L}$  after each iteration to avoid repetition.

The corresponding array response vectors for the selected path angles are used to form the analog precoding vectors

$$\mathbf{f}_i = \frac{1}{\sqrt{N_t}} \left[ 1, e^{j \frac{2\pi d_{\text{ant}}}{\lambda} \sin(\theta_{\mathcal{X}^{(i)}})}, \dots, e^{j \frac{2\pi d_{\text{ant}}}{\lambda} (N_t-1) \sin(\theta_{\mathcal{X}^{(i)}})} \right]^T, \quad (16)$$

$$\mathbf{w}_i = \frac{1}{\sqrt{N_r}} \left[ 1, e^{j \frac{2\pi d_{\text{ant}}}{\lambda} \sin(\phi_{\mathcal{X}^{(i)}})}, \dots, e^{j \frac{2\pi d_{\text{ant}}}{\lambda} (N_r-1) \sin(\phi_{\mathcal{X}^{(i)}})} \right]^T, \quad (17)$$

where  $\theta_{\mathcal{X}^{(i)}}$  and  $\phi_{\mathcal{X}^{(i)}}$  denote the AoD and AoA associated with the  $i$ -th selected path.

After  $N_t^{\text{RF}}$  and  $N_r^{\text{RF}}$  dominant directions are selected, the analog precoder and combiner are constructed as

$$\mathbf{F}_{\text{RF}} = [\mathbf{f}_1, \mathbf{f}_2, \dots, \mathbf{f}_{N_t^{\text{RF}}}], \quad (18)$$

$$\mathbf{W}_{\text{RF}} = [\mathbf{w}_1, \mathbf{w}_2, \dots, \mathbf{w}_{N_r^{\text{RF}}}], \quad (19)$$

#### B. Digital Precoder Design

The reduced-dimensional effective channel enables subcarrier-wise digital precoder design at much lower computational complexity. However, if a distinct digital precoder  $\mathbf{F}[k]$  is designed for every subcarrier, the receiver must feed back  $K$  digital precoding indices, leading to substantial overhead on the feedback channel.

Fortunately, due to the limited delay spread in mmWave systems, adjacent subcarriers often exhibit highly correlated channel responses [7], [8]. This frequency correlation can be leveraged to reduce feedback and design complexity by either clustering correlated subcarriers or interpolating digital precoders from a subset of anchor subcarriers.

In addition, we assume a shared codebook is pre-stored at both the transmitter and receiver to reduce the feedback overhead. To support large-scale antenna arrays, we adopt a shared Lloyd-trained codebook [6], [21] with  $B = 2^b$  unit-norm codewords, where  $b$  denotes the number of feedback bits per codeword index. Instead of feeding back full digital precoding matrices, the receiver only needs to transmit the index of the selected codeword, resulting in a feedback overhead of  $b$  bits per stream per reported subcarrier.

Given that each transmission involves  $N_s$  data streams, we must select  $N_s$  codewords from the codebook  $\mathcal{Q}$  to construct the digital precoder for each subcarrier.

Let  $\mathbf{H}^t$  denote the projected effective channel matrix at iteration  $t$ , initialized as  $\mathbf{H}^0 = \mathbf{H}_{\text{eff}}[k]$  defined in (10) for the target subcarrier. At each step, we adopt a greedy codeword selection strategy [6] to iteratively select the codeword that maximizes the projected channel gain

$$\mathbf{c}_t = \arg \max_{\mathbf{c} \in \mathcal{Q}} \|\mathbf{H}^t \mathbf{c}\|. \quad (20)$$

The selected codeword  $\mathbf{c}_t$  is appended to the digital precoder matrix

$$\mathbf{V}_k^t = [\mathbf{V}_k^{t-1}, \mathbf{c}_t], \quad (21)$$

where  $\mathbf{V}_k^0$  is initialized as an empty matrix. To suppress inter-stream interference, the effective channel is iteratively projected onto the orthogonal complement of previously selected codewords using QR decomposition.

This process iteratively suppresses correlation between selected directions. After  $N_s$  iterations, the digital precoder for the target subcarrier is given by

$$\mathbf{V}_q = \mathbf{V}_k^{N_s} \in \mathbb{C}^{N_t^{\text{RF}} \times N_s}, \quad (22)$$

where  $\mathbf{V}_q$  denotes the final digital precoding matrix for a selected anchor subcarrier.

## V. PROPOSED HIERARCHICAL INTERPOLATION

Conventional interpolation methods [8], [9] rely on fixed subband partitioning and fail to capture abrupt channel variations; to address this, we propose a binary-search-based hierarchical interpolation framework that enables adaptive subcarrier partitioning via efficient switching point detection.

We assume  $K$  subcarriers are uniformly partitioned into  $Q = K/M$  pilot intervals, where  $M$  denotes the pilot spacing. For each pilot tone, the receiver selects its digital precoder matrix  $\mathbf{V}_q = [\mathbf{v}_q^1, \dots, \mathbf{v}_q^{N_s}]$  from a shared codebook  $\mathcal{Q}$ .

Within each pilot interval, the  $k$ -th subcarrier ( $qM + 2 \leq m \leq (q+1)M$ ) selects its digital precoding matrix by comparing the gain of the left and right pilot codewords:

$$\mathbf{F}[m] = \arg \max_{\mathbf{V} \in \{\mathbf{V}_q, \mathbf{V}_{q+1}\}} \|\mathbf{H}_{\text{eff}}[m] \mathbf{V}\|. \quad (23)$$

This operation performs a local decision between adjacent codeword candidates. If the codewords selected at the two boundary pilot subcarriers are identical, all intermediate subcarriers reuse the same codeword. Otherwise, a binary search is performed to locate the switching point where the optimal codeword changes, avoiding exhaustive search.

The pseudo code of the proposed hierarchical interpolation is described in Algorithm 1.

Finally, to recover the transmitted signals, we apply linear equalization using either a zero-forcing (ZF) or minimum

---

### Algorithm 1: Proposed Binary-Search-Based Hierarchical Interpolation

---

**Input:** Pilot precoders  $\mathbf{V}_q = [\mathbf{v}_q^1, \dots, \mathbf{v}_q^{N_s}]$  for all pilot indices  $q = 0, 1, \dots, Q - 1$ ;  
Effective channels  $\mathbf{H}_{\text{eff}}[k]$  for all subcarriers  $k$ ;  
Codebook  $\mathcal{Q} = \{\mathbf{c}_j \in \mathbb{C}^{N_t^{\text{RF}} \times 1}\}$ ;  
Pilot spacing  $M$ , number of streams  $N_s$ ;  
Each pilot interval starts from  $\zeta_{\text{left}} = qM + 1$  and ends at  $\zeta_{\text{right}} = (q+1)M + 1$ .  
**Output:** Digital precoding matrices  $\mathbf{F}[k] \in \mathbb{C}^{N_t^{\text{RF}} \times N_s}$  for all  $k = 1, \dots, K$ .

```

1 for each pilot interval  $q = 0$  to  $Q - 1$  do
2   for each stream index  $t = 1$  to  $N_s$  do
3     if  $\mathbf{v}_q^t = \mathbf{v}_{q+1}^t$  then
4       for  $k = qM + 2$  to  $(q+1)M$  do
5         Assign  $\mathbf{F}[k][:, t] \leftarrow \mathbf{v}_q^t$ ;
6     else
7        $\zeta_{\text{left}} \leftarrow qM + 1$ ,  $\zeta_{\text{right}} \leftarrow (q+1)M + 1$ ;
8       while  $\zeta_{\text{right}} - \zeta_{\text{left}} > 1$  do
9          $\zeta_{\text{mid}} \leftarrow \lfloor \frac{\zeta_{\text{left}} + \zeta_{\text{right}}}{2} \rfloor$ ;
10        if  $\|\mathbf{H}_{\text{eff}}[\zeta_{\text{mid}}] \mathbf{v}_q^t\| > \|\mathbf{H}_{\text{eff}}[\zeta_{\text{mid}}] \mathbf{v}_{q+1}^t\|$ 
11          then
12             $\zeta_{\text{left}} \leftarrow \zeta_{\text{mid}}$ ;
13          else
14             $\zeta_{\text{right}} \leftarrow \zeta_{\text{mid}}$ ;
15         $\zeta^* \leftarrow \zeta_{\text{right}}$ ; // Switching point
16        from  $\mathbf{v}_q^t$  to  $\mathbf{v}_{q+1}^t$ 
17        for  $k = qM + 2$  to  $\zeta^* - 1$  do
18          Assign  $\mathbf{F}[k][:, t] \leftarrow \mathbf{v}_q^t$ ;
19        for  $k = \zeta^*$  to  $(q+1)M$  do
20          Assign  $\mathbf{F}[k][:, t] \leftarrow \mathbf{v}_{q+1}^t$ ;

```

---

mean square error (MMSE) combiner. These are defined as

$$\mathbf{W}_{\text{ZF}}[k] = \frac{\mathbf{F}^H[k] \mathbf{H}_{\text{eff}}^H[k]}{\mathbf{F}^H[k] \mathbf{H}_{\text{eff}}^H[k] \mathbf{H}_{\text{eff}}[k] \mathbf{F}[k]}, \quad (24)$$

$$\mathbf{W}_{\text{MMSE}}[k] = \frac{\mathbf{R}_s \mathbf{F}^H[k] \mathbf{H}_{\text{eff}}^H[k]}{\mathbf{H}_{\text{eff}}[k] \mathbf{F}[k] \mathbf{R}_s \mathbf{F}^H[k] \mathbf{H}_{\text{eff}}^H[k] + \mathbf{R}}, \quad (25)$$

where  $\mathbf{W}_{\text{ZF}}[k], \mathbf{W}_{\text{MMSE}}[k] \in \mathbb{C}^{N_s \times N_r^{\text{RF}}}$ ,  $\mathbf{R}_s$  and  $\mathbf{R}$  denote the signal and noise covariance matrices, respectively.

## VI. SIMULATION RESULTS

We consider a single-user mmWave MIMO-OFDM system with  $N_s = 2$ ,  $N_t = 128$ ,  $N_r = 32$ ,  $N_t^{\text{RF}} = 16$ ,  $N_r^{\text{RF}} = 12$ ,  $K = 2048$ ,  $M = 128$ ,  $L = 24$ , and  $D = 32$ , operating at 28 GHz under a geometric wideband mmWave channel model [3], [6].

For performance comparison, we consider the following four limited-feedback baselines:

- **Gaussian interpolation [9]**: Interpolates precoders across subcarriers using Euclidean-domain interpolation, but lacks adaptivity.
- **Geodesic interpolation [8]**: Performs interpolation on the Grassmannian manifold, improving accuracy but relying on fixed structures.
- **Simple clustering [11]**: Groups subcarriers into fixed clusters, offering low complexity but coarse adaptation.
- **SNR-maximizing clustering [11]**: Optimizes clusters based on SNR, achieving better performance at higher complexity.

#### A. Feedback Overhead Analysis

We quantify the feedback overhead of the proposed scheme and compare it with conventional per-subcarrier feedback. For a system with  $K = 2048$  subcarriers and a  $b = 5$ -bit codebook, conventional schemes require  $Kb = 10240$  bits to feed back digital precoding indices.

In contrast, the proposed hierarchical interpolation requires feedback only at pilot subcarriers and additional binary-search decisions within each interval. Specifically, the feedback overhead scales as  $(K/M + \log_2 M)b$ , where  $M$  denotes the pilot spacing. With  $M = 128$ , this corresponds to  $(16+7) \times 5 = 115$  bits. This reduction is achieved by exploiting frequency-domain correlation and adaptively detecting codeword switching points via binary search, rather than assigning precoders independently for each subcarrier.

Therefore, the proposed scheme achieves a feedback reduction of more than 98%, demonstrating its effectiveness for wideband mmWave systems.

#### B. Spectral Efficiency Performance

Fig. 2 illustrates the spectral efficiency performance of different precoding schemes across a wide SNR range. All methods achieve comparable achievable rates, indicating that the proposed hierarchical interpolation preserves most of the spectral efficiency despite significantly reduced feedback overhead.

At high SNR, the proposed method slightly outperforms conventional interpolation schemes. This improvement is attributed to its ability to adaptively detect codeword switching points within each pilot interval, thereby achieving more accurate subcarrier-wise precoder assignment compared to fixed-interval methods.

These results demonstrate that the proposed scheme achieves a favorable tradeoff between feedback overhead reduction and spectral efficiency.

#### C. BER Performance

Fig. 3 compares the BER performance of different precoding schemes under QPSK modulation and perfect CSI conditions. The proposed hierarchical interpolation achieves the lowest BER across all SNR values. This gain is attributed to its adaptive subcarrier partitioning enabled by binary search, which improves codeword selection accuracy.

In contrast, Gaussian interpolation [9] and geodesic interpolation [8] rely on fixed interpolation structures and therefore

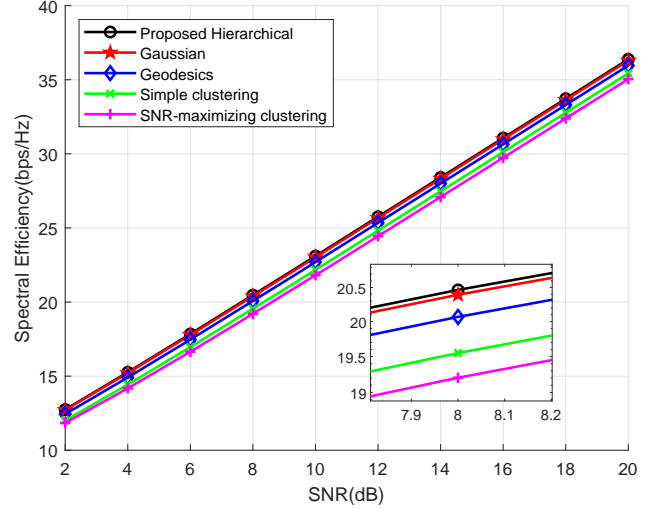


Fig. 2: Spectral efficiency comparison of different precoding schemes.

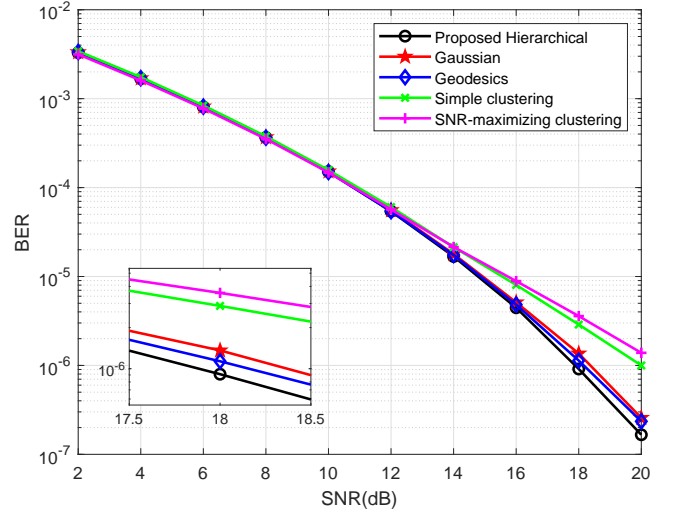


Fig. 3: Average BER performance of different precoding schemes.

fail to capture abrupt channel variations. Clustering-based approaches [11] suffer from coarse grouping, which reduces spatial diversity and leads to degraded error performance.

These results indicate that the proposed method maintains reliable error performance while significantly reducing feedback overhead.

#### D. Computational Complexity

We compare the computational complexity in terms of the average runtime per Monte Carlo realization.

Table I shows that the proposed hierarchical interpolation achieves the lowest computational complexity among all compared methods. Specifically, it is about  $7.8 \times$  faster than Gaussian interpolation [9] and  $2.2 \times$  faster than geodesic interpolation [8]. Compared with SNR-maximizing clustering [11], the proposed method reduces computation time by more than

TABLE I: Computation Time of Different Precoding Algorithms

Method	Average time (s)
SNR-maximizing clustering [11]	$2.6 \times 10^{-1}$
Simple clustering [11]	$2.3 \times 10^{-3}$
Gaussian interpolation [9]	$5.2 \times 10^{-3}$
Geodesic interpolation [8]	$1.5 \times 10^{-3}$
Proposed hierarchical interpolation	$6.7 \times 10^{-4}$

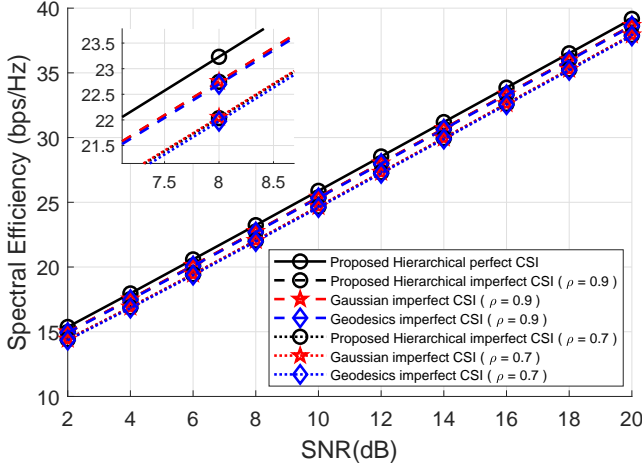


Fig. 4: Spectral efficiency comparison under perfect and imperfect CSI conditions.

two orders of magnitude. This efficiency gain is attributed to the logarithmic-time binary search structure, which reduces the number of effective channel evaluations from  $\mathcal{O}(K)$  in conventional schemes to  $\mathcal{O}\left(\frac{K}{M} \log_2 M\right)$ .

Overall, the proposed method achieves a favorable trade-off among computational complexity, spectral efficiency, and feedback overhead, making it suitable for real-time wideband mmWave systems.

#### E. Performance Under Imperfect CSI

We evaluate the robustness of the proposed scheme under imperfect CSI, where the estimated channel is modeled as  $\mathbf{H}_{\text{est}}[k] = \rho \mathbf{H}_{\text{eff}}[k] + \sqrt{1 - \rho^2} \mathbf{H}_{\text{err}}[k]$ , with  $\mathbf{H}_{\text{err}}[k] \sim \mathcal{CN}(0, 1)$ .

Fig. 4 compares spectral efficiency under perfect and imperfect CSI. The proposed method outperforms Gaussian and geodesic interpolation across all SNRs, with only minor degradation at  $\rho = 0.7$ , demonstrating robustness due to hierarchical interpolation and codebook design.

### VII. CONCLUSION

In this paper, we propose a feedback-efficient hybrid precoding framework for wideband mmWave MIMO-OFDM systems. Analog precoders are constructed from dominant AoA/AoD components, and a Lloyd-based codebook enables limited-feedback digital precoding. A binary-search-based hierarchical interpolation scheme achieves sub-linear feedback scaling with over 98% reduction, while maintaining spectral efficiency and robustness under imperfect CSI.

### REFERENCES

- [1] M. F. Haider, F. You, S. He, T. Rahkonen, and J. P. Aikio, "Predistortion-based linearization for 5G and beyond millimeter-wave transceiver systems: A comprehensive survey," *IEEE Commun. Surveys Tuts.*, vol. 24, no. 4, pp. 2029–2072, Aug. 2022.
- [2] R. W. H. Jr., N. Gonzalez-Prelcic, S. Rangan, W. Roh, and A. M. Sayeed, "An overview of signal processing techniques for millimeter wave MIMO systems," *IEEE J. Sel. Top. Signal Process.*, vol. 10, no. 3, pp. 436–453, Apr. 2016.
- [3] O. E. Ayach, S. Rajagopal, S. Abu-Surra, Z. Pi, and R. W. Heath, "Spatially sparse precoding in millimeter wave MIMO systems," *IEEE Trans. Wirel. Commun.*, vol. 13, no. 3, pp. 1499–1513, Mar. 2014.
- [4] X. Gao, L. Dai, S. Han, C.-L. I, and R. W. Heath, "Energy-efficient hybrid analog and digital precoding for mmWave MIMO systems with large antenna arrays," *IEEE J. Sel. Areas Commun.*, vol. 34, no. 4, pp. 998–1009, Apr. 2016.
- [5] Y.-C. Wang, P.-H. Chou, and C.-D. Chung, "Circulantly precoded OFDM," in *Proc. IEEE/CIC Int. Conf. Commun. China (ICCC)*, Jul. 2016, pp. 1–6.
- [6] A. Alkhateeb and R. W. Heath, "Frequency selective hybrid precoding for limited feedback millimeter wave systems," *IEEE Trans. Commun.*, vol. 64, no. 5, pp. 1801–1818, May 2016.
- [7] J. Choi and R. W. H. Jr., "Interpolation based transmit beamforming for MIMO-OFDM with limited feedback," *IEEE Trans. Signal Process.*, vol. 53, no. 11, pp. 4125–4135, Nov. 2005.
- [8] T. Pande, D. J. Love, and J. V. Krogmeier, "Reduced feedback MIMO-OFDM precoding and antenna selection," *IEEE Trans. Signal Process.*, vol. 55, no. 5, pp. 2284–2297, May 2007.
- [9] C. He, P. Zhu, B. Sheng, and X. You, "Two novel interpolation algorithms for MIMO-OFDM systems with limited feedback," in *Proc. IEEE Veh. Technol. Conf. (VTC-Fall)*, Sep. 2011, pp. 1–5.
- [10] L. Wang, B. Sheng, and C. He, "Study on feedback reduction techniques in MIMO-OFDM beamforming systems," in *Proc. Int. Conf. Wireless Commun. Signal Process. (WCSP)*, Oct. 2012, pp. 1–5.
- [11] M. Wu, C. Shen, and Z. Qiu, "Feedback reduction based on clustering in MIMO-OFDM beamforming systems," in *Proc. IEEE Int. Conf. Wireless Commun., Netw., Mobile Comput. (WiCOM)*, Sep. 2009, pp. 1–4.
- [12] B. Mondal and R. W. H. Jr., "Algorithms for quantized precoding in MIMO OFDM beamforming systems," in *Proc. SPIE: Noise Commun. Syst.*, vol. 5847, Oct. 2005, pp. 80–87.
- [13] K. Wei, J. Xu, W. Xu, N. Wang, and D. Chen, "Distributed neural precoding for hybrid mmWave MIMO communications with limited feedback," *IEEE Commun. Lett.*, vol. 26, no. 7, pp. 1568–1572, Jul. 2022.
- [14] Q. Xue, C. Dong, X. Li, J. Yi, and K. Niu, "Integrated deep implicit CSI feedback and beamforming design for FDD mmWave massive MIMO systems," *IEEE Wireless Commun. Lett.*, vol. 12, no. 1, pp. 119–123, Jan. 2023.
- [15] L. Zhao, H. Xu, Z. Wang, X. Chen, and A. Zhou, "Joint channel estimation and feedback for mm-Wave system using federated learning," *IEEE Commun. Lett.*, vol. 26, no. 8, pp. 1819–1823, Aug. 2022.
- [16] S. Zhang, S. Zhang, J. Ma, T. Liu, and O. A. Dobre, "Deep learning based antenna-time domain channel extrapolation for hybrid mmwave massive MIMO," *IEEE Trans. Veh. Technol.*, vol. 71, no. 12, pp. 13398–13402, Dec. 2022.
- [17] M. Wu, Z. Gao, Z. Gao, D. Wu, Y. Yang, and Y. Huang, "Deep learning-based hybrid precoding for FDD massive MIMO-OFDM systems with a limited pilot and feedback overhead," in *Proc. IEEE Int. Conf. Commun. Workshops (ICC Wkshps)*, May 2022, pp. 318–323.
- [18] Y. Sun, H. Wang, M. Yuan, T. Zhu, and A. Kawoya, "Training-based hybrid precoding scheme for multiuser massive MIMO-OFDM," *IEEE Commun. Lett.*, vol. 25, no. 11, pp. 3729–3732, Nov. 2021.
- [19] A. Alkhateeb, G. Leus, and R. W. Heath, "Limited feedback hybrid precoding for multi-user millimeter wave systems," *IEEE Trans. Wirel. Commun.*, vol. 14, no. 11, pp. 6481–6494, Nov. 2015.
- [20] A. V. Oppenheim and R. W. Schaffer, *Discrete-Time Signal Processing*, 2nd ed. Prentice Hall, 1999.
- [21] J. Linde, A. Buzo, and R. Gray, "An algorithm for vector quantizer design," *IEEE Trans. Commun.*, vol. 28, no. 1, pp. 84–95, Jan. 1980.